Springer

Journal of Mechanical Science and Technology 22 (2008) 1896~1901

Journal of Mechanical Science and Technology

www.springerlink.com/content/1738-494x
DOI 10.1007/s12206-008-0729-6

Performance characteristics of turbo blower in a refuse collecting system according to operation conditions †

C.-M. Jang[1,*], D.-W. Kim[1] and S.-Y. Lee[2]

[1]*Fire & Engineering Services Research Dept., Korea Institute of Construction Technology, 2311, Daehwa-dong, Goyang-Si, 411-712, Korea*
[2]*ANST, 806 Daerung Post Tower Ⅲ 182-4 Guro-Dong, Guro-Gu, Seoul, 152-847, Korea*

(Manuscript Received April 16, 2008; Revised July 1, 2008; Accepted July 23, 2008)

Abstract

A simulator for a refuse collecting system is designed to investigate the performance characteristics of a turbo blower operating at different rotational frequencies. The simulator consists of an air intake, a waste chute, circular duct, waste collector and turbo blower. Experimental measurements and numerical simulation with three-dimensional Navier-Stokes equations have been performed to analyze the performance of the turbo blower. Throughout numerical simulation of the simulator, it is found that the input energy of the blower can be reduced by controlling the rotational frequency of impeller while the efficiency of the blower keeps constant. The required outlet pressure and flow rate of the blower can be also adjusted along the system resistance of the refuse collecting system. Detailed flow characteristics inside the blower are analyzed for different rotational frequencies.

Keywords: Turbo blower; Refuse collecting system; Efficiency; Numerical simulation; System resistance curve

1. Introduction

A turbo blower is commonly used to increase suction pressure in a refuse collecting system.[1, 2] Required suction pressure of a turbo blower depends on the length of a pipeline and the diameter of pipe. Three or four blowers are installed in the terminal station serially for making high suction pressure. The operation of a turbo blower in a refuse collecting system can be divided into two methods: one is a simple on-off operation of a blower and the other is a control of blower's rotational frequency partly with on-off operation of a blower. In the view point of energy saving, the control of the rotational frequency of an impeller would be more effective than the simple on-off operation of a blower. Until now, theoretical analysis for the operation of a turbo blower used in the refuse collecting system is not reviewed.

In the present study, performance characteristics of a turbo blower installed in the refuse collecting system are analyzed by experimental measurements and numerical simulation with three-dimensional Navier-Stokes equations. Blower performance is analyzed according to the rotational frequency of impeller while the flow rate is set by the local value of a system resistance. Detailed analysis of internal flow of the blower is also performed using the results of numerical simulation.

2. Modeled refuse collecting system and test fan

In the present study, a modeled refuse collecting system is introduced to analyze the flow characteristics inside the system and to design each component used in the system, as shown in Fig. 1. The system

† This paper was presented at the 9th Asian International Conference on Fluid Machinery (AICFM9), Jeju, Korea, October 16-19, 2007.

*Corresponding author. Tel.: +82 31 369 0508, Fax.: +82 31 369 0540
E-mail address: jangcm@kict.re.kr

Table 1. Design specification of test blower.

Name	Value
Flow Coefficient	0.21
Pressure Coefficient	1.12
Rotational Frequency of Impeller	3550 rpm
Tip Diameter of Impeller	565 mm
Number of Blade	8 EA
Blade Type	Radial

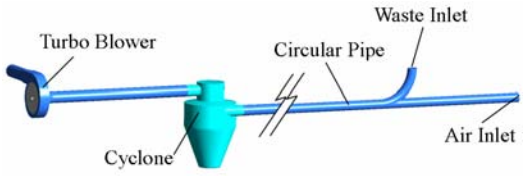

(a) Modeled system

(b) Turbo blower

Fig. 1. Configuration of a modeled refuse collecting system.

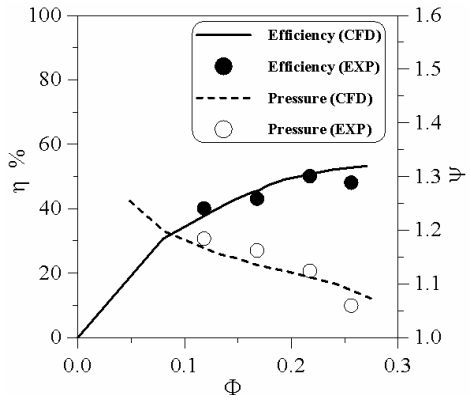

Fig. 2. Performance curves of a turbo blower operating at 3550 rpm.

consists of an air intake, a waste chute, circular duct, waste collector and turbo blower. The inner diameter of the circular duct is 204.7 mm, which is modeled from the real piping system having a diameter between 400 and 600 mm. The total length of the system is about 80 m.

Turbo blower having a radial typed blade is designed and tested. Design specifications of the rotor blade are summarized in Table 1. A flow coefficient (Φ) and a static pressure rise coefficient (Ψ) are defined as

$$\Phi = \frac{Q}{A\,U_t} \tag{1}$$

$$\Psi = \frac{2\,\Delta P_S}{\rho\,U_t^{\,2}} \tag{2}$$

where Q is the volume flow rate, ΔP_S is the static pressure rise, U_t is the rotor tip speed, ρ is the density, and A is the outlet area of the turbo blower.

Fig. 2 shows the performance characteristics of the test fan operating at the rotor rotational speed of 3550 rpm. Whereas the measuring position of static pressure at the upstream of the blower is the inlet of the blower, the position at the downstream is 1.4 m from the exit of the blower. The efficiency η is defined using the static pressure rise as

$$\eta = \frac{Q \cdot \Delta P_t}{P_{input}} \tag{3}$$

where ΔP_t is the total pressure rise and P_{input} is the input power of a driving motor.

3. Numerical analysis method

To analyze three-dimensional flow field in the turbo blower operating at the different rotational frequencies of a rotor blade, general analysis code, CFX-10 [3], is employed in the present work. In present numerical simulation, the flow field was simulated in the frame of reference rotating with the impeller.

The numerical method used in the present simulation is outlined in the following.

Incompressible Reynolds-Averaged Navier-Stokes equations (RANS) and continuity equation are introduced for the present steady flow calculation. The governing equations are analyzed using a finite volume approximation. Discretizations of convection

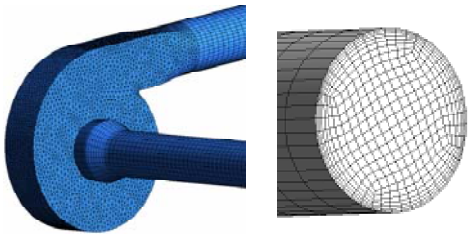

(a) Surface mesh of turbo blower and duct inlet region

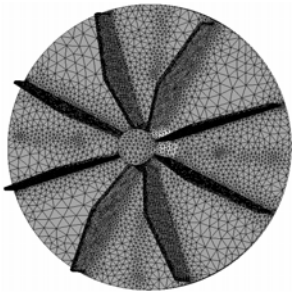

(b) Surface mesh on the rotor blade

Fig. 3. Computational grid of a turbo blower.

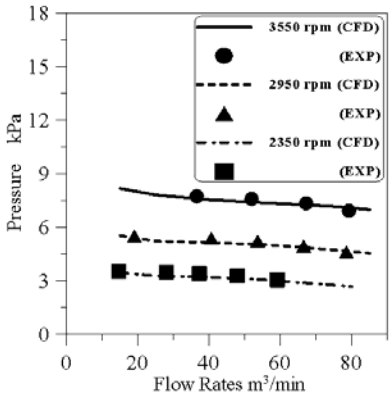

Fig. 4. Comparisons of numerical and experimental results for different rotational frequencies of a rotor.

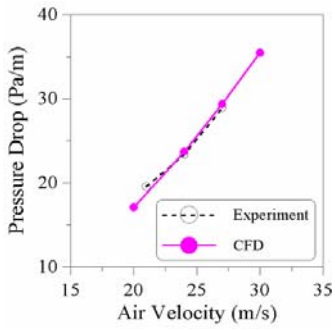

Fig. 5. Comparisons of numerical and experimental results of pressure drop in a circular duct.

and diffusion terms of the equations are adopted by modified upwind scheme and central difference scheme, respectively. Standard k-ε turbulence model [4] with scalable wall function is employed to estimate the eddy viscosity.

Fig. 3 shows computational grids of the turbo blower. Unstructured grids are used to represent a composite grid system, and the whole grid system has about 1,200,000 nodes. It is noted that tetra-prism mesh imposes in the turbo blower and the cyclone whereas hexa mesh is applied to the circular pipe region with an O-grid mesh to enhance the grid performance.

As boundary conditions, atmospheric pressure is specified at the inlet and outlet. Inlet turbulence intensity is assumed to be 5 percent. No-slip and adiabatic wall conditions are used on blade, casing and hub surfaces.

4. Results and discussions

4.1 Validation of numerical analysis

For the validation of the numerical solutions, the

Table 2. Performance of turbo blower at different operating conditions.

Position in Fig. 6	Flow Rates (m^3/min)	Rotational Frequency (rpm)	Pressure (kPa)	Efficiency (%)
A	64.5	3550	7.3	49.5
B	53.9	2950	5.1	49.4
C	42.5	2350	3.2	49.2

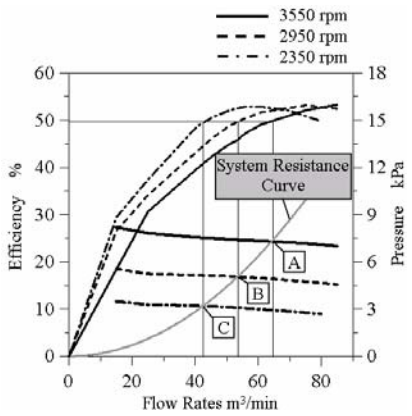

Fig. 6. Comparisons of blower efficiency for three different rotational frequencies of rotor blade along the system resistance.

distributions of blower efficiency and pressure are compared to the experimental results at the design and off design conditions, as shown in Fig. 2. In the figure, the solid and broken lines imply the results obtained by numerical simulation.

The figure shows that the distributions of the blower efficiency and the pressure obtained by numerical simulation match well with the experimental results. The maximum difference between the computational and experimental result at the design flow rate is observed at the flow coefficient of 0.255, and is 5 percent based on the numerical data.

Fig. 4 shows the comparison between computational and experimental distributions of pressure with respect to mass flow rate for three different rotational frequencies: that is, 3550, 2950 and 2350 rpm. The comparisons between the numerical and experimental results at the design and off design flow rates show that the pressure of the turbo blower rotor is simulated correctly by the present calculation.

Pressure drop obtained by numerical simulation is compared to that determined by experiments in Fig. 5. The pressure drop is normalized by unit length of a circular duct and represents according to air velocity inside the duct. Relatively good agreements between the experimental and numerical results are observed.

In the following, the performance and flow characteristics of the turbo blower are analyzed using numerical results in detail.

4.2 Operation of turbo blower

As shown in Fig. 1, the turbo blower used in the refuse collecting system is connected by a circular duct with a cyclone and a circular duct. In the field system, three or four turbo blowers are used to increase a suction pressure. When high suction pressure is needed, all blowers installed in the system are connected by a serial pattern. The level of the suction pressure is mainly determined by the distance between a turbo blower and a waste inlet and a diameter of a circular duct. In usual, the distance reaches about 2.0 km when the diameter of circular duct is about 500 mm. The number of turbo blower is determined by the required suction pressure in a refuse collecting system.

In the operation of a turbo blower, it can be considered two operation methods. One is a simple on-off operation for each turbo blower according to the level of suction pressure needed. The other is the changing the blower's rotational frequency partly with on-off operation of the blower. In the present study, the latter one is considered because it can be reduced the input power effectively to operate turbo blowers.

Fig. 6 shows the performance curves of the turbo blower operating at three different rotation conditions, which is the result of numerical simulation. In the figure, gray and solid line represents a system resistance curve of the system shown in Fig. 1(a).

Three operating points, that is "A", "B", and "C" in Fig. 6, are determined at the intersection positions between system resistance curve and each pressure line. The values of flow rates, pressure and efficiency at the three rotational frequencies of impeller are shown in Table 2. The efficiency at the three operating points, which is on the system resistance curve, has almost same value although the flow rates and pressure are different. It should be noticed that the blower efficiency is not changed if the blower is operating along the system resistance curve. In operation of the turbo blower for the refuse collecting system, the input energy of the blower can be reduced by controlling the rotational frequency of impeller while pressure is adjusted to flow rate along the line of system resistance of the refuse collecting system.

In the refuse collecting system, a lot of waste inlets shown in Fig. 1(a) are installed along the main circular pipe. Required pressure for each waste inlet is mainly determined by the distance from the turbo blower.

Table 3. Mean velocity inside the piping system according to different operating conditions.

Position in Fig. 6	Inner diameter of duct (mm)	Flow rates (m^3/min)	Mean velocity (m/s)
A	204.7	64.5	32.6
B		53.9	27.0
C		42.5	21.5

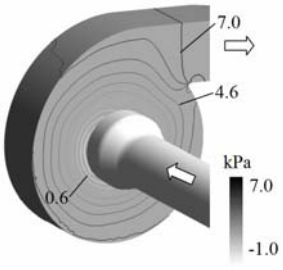

Fig. 7. Pressure distribution on the casing of a turbo blower operating at 3550 rpm. (contour intervals = 0.8 kPa).

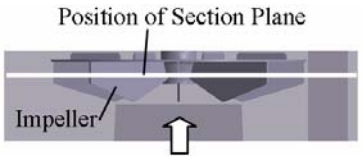

(a) Position of observing plane

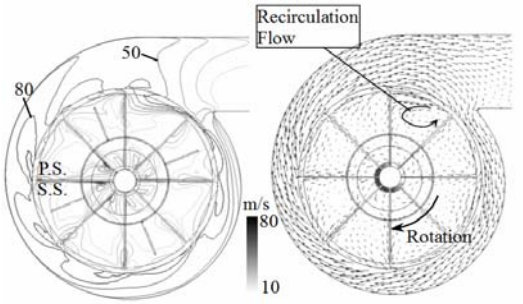

(b) Velocity contours (contour intervals = 10 m/s) and velocity vectors in the frame of reference rotating with a impeller

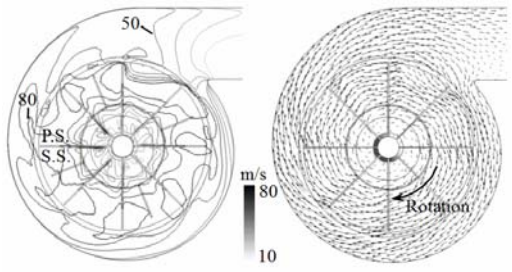

(c) Velocity contours (contour intervals = 10 m/s) and velocity vectors in the stationary frame

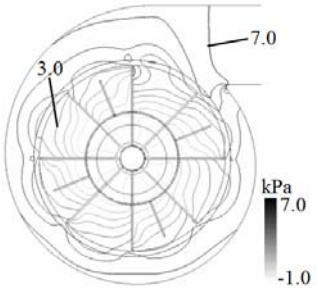

(d) Pressure contours (contour intervals = 0.8 kPa)

Fig. 8. Distributions of velocity and pressure on the plane parallel to the impeller plate of the turbo blower rotating at 3550 rpm.

It can be considered that the positions of "A", "B", and "C" in Fig. 6 are the required pressure for different positions of waste inlets. Therefore the input power of the turbo blower can be reduced by changing the rotational frequency of impeller from position "A" to "C", which has constant blower efficiency along the system resistance curve.

Mean velocity inside the circular pipe for the three positions of "A", "B" and "C" is shown in Table 3. It is noted that higher pressure requires as the air velocity increases as shown in Fig. 5.

4.3 Flow characteristics inside the impeller of turbo blower operating at different rotational frequencies

Flow characteristics inside the turbo blower are analyzed by the results of three-dimensional numerical simulation.

Fig. 7 shows pressure distribution on the casing of a turbo blower operating at 3550 rpm. It can be understood that inlet suction pressure having a minus value recovers as the flow moves downstream due to the angular momentum generated by the turbo blower.

Distributions of velocity and pressure on the plane parallel to the impeller plate of the turbo blower rotating at 3550 rpm are shown in Fig. 8. The position of observing plane presents in Fig. 8(a), which is perspective view from top casing.

As shown in velocity vectors in the frame of reference rotating with an impeller of Fig. 8(b), a large recirculation flow is formed in the blade passage located near the cutoff of casing.

In the stationary frame, an inward radial flow is observed where the recirculation is formed. The strong radial flow caused by a reverse flow due to the high pressure above the cutoff is observed as shown in Fig. 8(d).

A strong the radial flow near the suction and pressure surfaces of impeller is also observed in Fig. 8(b). A gradual pressure increase shows along the rotation of impeller from the cutoff position to the outlet of a blower.

Fig. 9 shows the distributions of velocity and pressure on the sectional plane of the turbo blower operating at three different conditions. The position of the plane is located at the outlet of the turbo blower as

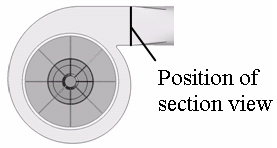

(a) Position of plane

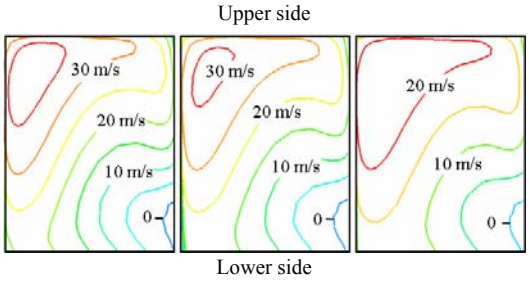

(b) Velocity contours (contour intervals = 5)

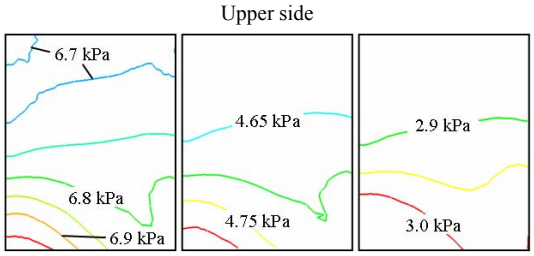

(c) Pressure contours (contour intervals = 0.5)

3550 rpm 2950 rpm 2350 rpm

Fig. 9. Distributions of velocity and pressure on the sectional plane of a turbo blower operating at three different operating conditions.

shown in Fig. 9(a). Relatively high velocity is observed at the left corner of upper side for three cases, which is mainly caused by the strong centrifugal force by a rotating impeller. The high velocity having a strong rotational component makes radial flow toward to the impeller near the cutoff region as shown in Fig. 8(b) and 8(c).

In the lower side of the flow passage at the outlet, a reverse flow is also observed at the right corner. In the outlet plane, relatively high pressure is distributed at the lower side which is caused by the retarded velocity. As shown in Fig. 9, the distributions of velocity and pressure have almost same pattern for three rotational frequencies although the absolute value of each variable is different.

5. Conclusion

Performance characteristics of a turbo blower installed in the refuse collecting system are analyzed by experimental measurements and numerical simulation with three-dimensional Navier-Stokes equations. In the system, the input energy of a turbo blower can be reduced by controlling the rotational frequency of impeller while the efficiency of the blower keeps constant. The required outlet pressure and flow rate of the blower can be also adjusted along the system resistance of the system. It is noted that the blower efficiency is constant along the system resistance curve of refuse collecting system.

It is found that a large recirculation flow is formed in the blade passage located near the cutoff of casing. The high velocity having a strong rotational component makes radial flow towards to the impeller near the cutoff region, thus makes a recirculation flow.

References

[1] S.-C. Lin and C.-L. Huang, An Integrated Experimental and Numerical Study of Forward-Curved Centrifugal Fan, Experimental Thermal and Fluid Science, 26 (2002) 421-434

[2] N. N. Bayomi, A. Abdel Hafiz and A. M. Osman, Effect of inlet straighteners on Centrifugal Fan Performance, Energy Conversion & Management, 547 (2006) 3307-3318.

[3] CFX-10 User Manual, Ansys Inc., (2005).

[4] L. Prandtl, On the Fully Developed Turbulence, *J. Applied Math. & Mech*., 5 (1925) 136-139.